Frequency Modulation in a Submillimeter-Wave Gyrotron

T. Idehara, M. Pereyaslavets, N. Nishida, and K. Yoshida
Department of Applied Physics, Faculty of Engineering, Fukui University, Bunkyo 3-9-1, Fukui 910-8507, Japan

I. Ogawa
Cryogenic Laboratory, Faculty of Engineering, Fukui University, Bunkyo 3-9-1, Fukui 910-8507, Japan
(Received 26 January 1998)

A first demonstration has been made of frequency modulation of a gyrotron output signal. The experiment was performed on a submillimeter-wave gyrotron operating near 300 GHz. The modulation amplitude of several tens of MHz has been achieved by a 120 V modulation of the accelerating voltage; this results in variation of the relativistic electron mass and corresponding variation in the electron cyclotron frequency f_c. The observed modulation of the output frequency is 2.3 times smaller than the variation in f_c. There is reasonable agreement between the experimental results and a simulation employing the energy transfer formula in a cavity. [S0031-9007(98)06878-1]

PACS numbers: 84.40.Ik

Gyrotrons are practically the only sources of medium power radiation in the submillimeter-wave region [1,2]. Frequency and amplitude modulations of gyrotrons are important for their new applications in various areas [3,4,14], like remote sensing of atmosphere, submillimeter-wave telecommunications, studies of relaxation processes in plasmas and other materials, phase sensitive detection of the scattered signal from a plasma, and so on. While some research [5–7] has been carried out for the amplitude modulation of gyrotron, there are no results regarding its frequency modulation. Generally, it is difficult to modulate the frequency, because a gyrotron operates at fixed frequencies determined by the fixed geometry of its high-Q cavity. For example, in our gyrotron the total Q including Ohmic losses is $Q = 5800$. The relatively slow change of gyrotron frequency has been performed in several papers [8–12,15–19] by variation in the external magnetic field. However, as it was pointed out in [13,14], the typical time scale of variation in the magnetic field is of the order of 0.1 s. Hence, a modulation of the operating voltage was theoretically considered in [13,14] to achieve much faster frequency change of the gyrotron output signal. Quasistatic gyrotron frequency pulling by variation in anode and beam voltages was implemented, e.g., in [15–19].

In this Letter we describe the first results for a rapid (up to 40 kHz) frequency modulation of gyrotron output.

A submillimeter-wave gyrotron designed in the framework of "Gyrotron FU" series at the Fukui University was employed for our frequency modulation experiment. It was Gyrotron FU IV [1] with the following typical operation parameters: the beam energy $eV_c = 16.5$ keV, the beam current $I_b = 0.16$ A, the static magnetic field intensity $B_0 = 11$ T, the output frequency $f_r = 302$ GHz, and the output power $P = 20$ W. The gyrotron was operated completely in continuous wave (cw) mode.

The gyrotron operating frequency ω_r is usually either near the cyclotron frequency ω_c or near one of its harmonics $n\omega_c$, where $\omega_c = eB_0/(\gamma m_0)$; e and m_0 are the electric charge and the rest mass of electron, respectively. The relativistic factor $\gamma = (1 - v^2/c^2)^{-1/2}$ is determined by the accelerating voltage V since $(\gamma - 1)m_0c^2 = eV$. Obviously, variation in V changes γ and the relativistic electron mass. Therefore, the cyclotron frequency ω_c is, in its turn, modulated, and the output gyrotron frequency ω_r is modulated as well, despite restrictions imposed by the cavity on operating frequency flexibility.

The beam energy in Gyrotron FU IV is modulated by variation in the body potential. The body includes the cavity and is separated electrically from the beam collector by a ceramic insulator. The experimental setup is shown in Fig. 1.

The output power is transmitted by circular waveguides and emitted to a horn antenna. The frequency is measured by a heterodyne detection system consisting of a sweep oscillator, a frequency counter, a harmonic mixer, and a modulation domain analyzer. The block diagram is presented in Fig. 2. The detected signal is mixed with a high harmonic of the local oscillator. The time and frequency resolutions of the detection system are 10 μs and 10 kHz, respectively. A typical result of the frequency modulation experiment is shown in Fig. 3. The left-hand side trace corresponds to the variation of the output frequency and the right-hand side trace to the modulation of the body potential. The peak-to-peak value of the body potential modulation is 120 V, the body potential is modulated with the frequency $f_m =$ 15 kHz, and the peak-to-peak amplitude of the output frequency modulation is $\Delta f = 30$ MHz, i.e., almost equal to the linewidth of the gyrotron cavity. The higher beam energy corresponds to the lower measured output frequency, so there is qualitative correspondence with variation in the electron cyclotron frequency. The left-hand side spectrum analyzer trace in Fig. 4 presents the frequency spectrum of the output signal without frequency modulation and the right-hand side trace with the frequency

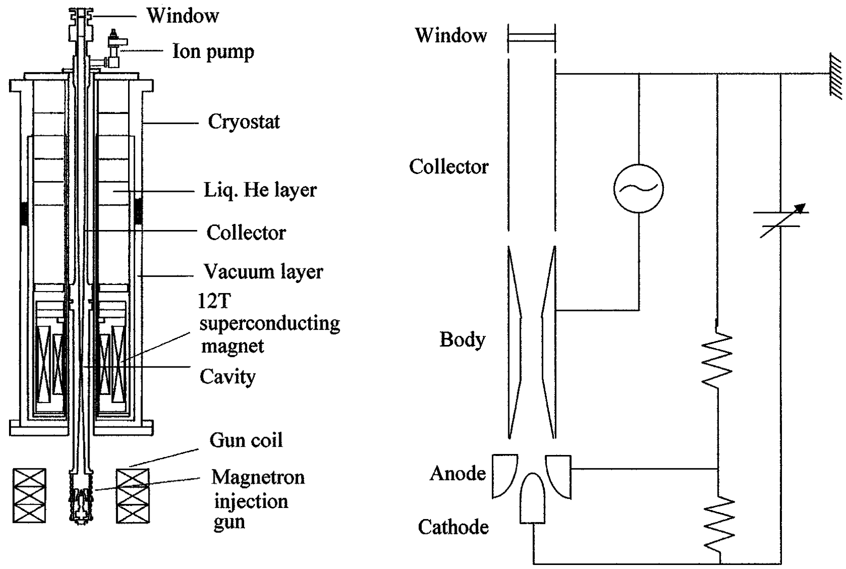

FIG. 1. Experimental setup for Gyrotron FU IV.

modulation. The frequency width δf of the gyrotron output itself in the left-hand side trace is about 100 kHz. A well-known pattern of a frequency spectrum under modulation is obvious in the right-hand side trace. The frequency width δf of the spectrum is in good agreement with the amplitude Δf of the frequency modulation determined from the f_{IF} trace in Fig. 4. The corresponding V_b modulation with the amplitude of 120 V is also plotted in Fig. 4. The frequency modulation amplitude Δf versus the body potential modulation amplitude ΔV_b is plotted in Fig. 5 for several values of f_m. There is an almost linear dependence between Δf and ΔV_b for all values of f_m. A data scatter in Fig. 5 increases when the frequency modulation amplitude approaches the gyrotron cavity linewidth. The efficiency of frequency modulation shown in Fig. 5 is $\Delta f/\Delta V_b = 0.247 \pm 0.06$ MHz/V. The estimated cyclotron frequency variation versus ΔV_b is easily calculated as $\Delta f_c/\Delta V_b = 0.570$ MHz/V; i.e., the observed modulation efficiency $\Delta f/\Delta V_b$ is 2.3 times smaller than $\Delta f_c/\Delta V_b$. Since flexibility of the gyrotron operating frequency ω_r is restricted by its high-Q cavity ($Q = 5800$), such a difference between $\Delta f/\Delta V_b$ and $\Delta f_c/\Delta V_b$ could be expected.

To compute the frequency modulation, we should define the complex energy transfer from the electrons to the microwave field in the gyrotron cavity as

$$P_a(V) = -e \int_{z_{\min}}^{z_{\min}+L} \vec{E}(z, r, \Phi) \exp[j(\omega_r t + \theta)] \cdot \frac{d\vec{s}}{dt} \frac{dt}{dz} dz, \quad (1)$$

where $\vec{E}$ is the microwave electrical field in the cavity, t is the time, and $\vec{s}$ describes the electron helical trajectory as

$$\frac{ds_{x,y}}{dt} = \begin{cases} v_\perp \cos[\omega_c(t - z_{\min}/v_\parallel) + \varphi] \\ v_\perp \sin[\omega_c(t - z_{\min}/v_\parallel) + \varphi] \end{cases}. \quad (2)$$

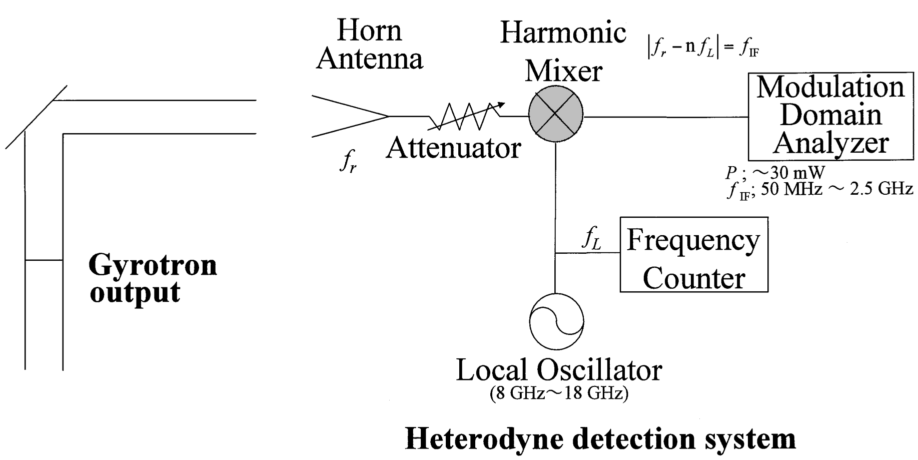

FIG. 2. Frequency measurements system with the resolutions 10 μs for time and 10 kHz for frequency.

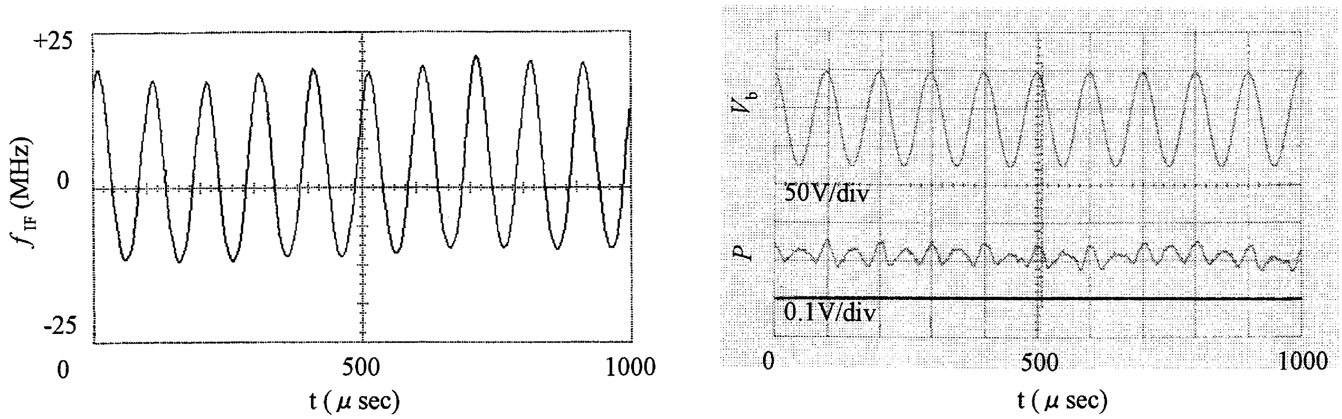

FIG. 3. Measured frequency modulation and the variations of body potential V_b and output power P. TE_{031} cavity mode, frequency $f_r = 301.99$ GHz, beam energy $eV_c = 16.5$ keV, beam current $I_b = 0.155$ A, $f_m = 10$ kHz; frequency modulation amplitude $\Delta f = 30$ MHz, and amplitude of body potential modulation $\Delta V_b = 120$ V.

Here $v_\parallel$ and $v_\perp$ are the electron velocities along the cavity axis Oz and in the cross-section plane, whereas the angles θ and φ define the phases of the microwave field and the electron rotation, respectively. Following [20], the amplitude of frequency modulation caused by $\Delta V_b = V_1 - V_2$ is

$$\Delta f = f_1 - f_2 = \frac{f_{\rm res}}{2Q_{\rm tot}}\left[\frac{\mathrm{Im}\{P_a(V_1)\}}{\mathrm{Re}\{P_a(V_1)\}} - \frac{\mathrm{Im}\{P_a(V_2)\}}{\mathrm{Re}\{P_a(V_2)\}}\right], \quad (3)$$

where $Q_{\rm tot}$ is the cavity quality factor. The result of Eq. (3) heavily depends on θ and φ. We can limit ourselves with $\theta = 0$ and $\theta = \pi/2$, since a rotating electromagnetic field with an arbitrary phase can be represented as a linear combination of those two fields.

Obviously, the contribution of electrons with various φ is different and one can define an effective electron rotation phase $\varphi_{\rm eff}$ giving the correct value of frequency modulation for an average electron trajectory. The electron rotation phases φ are described by an electron

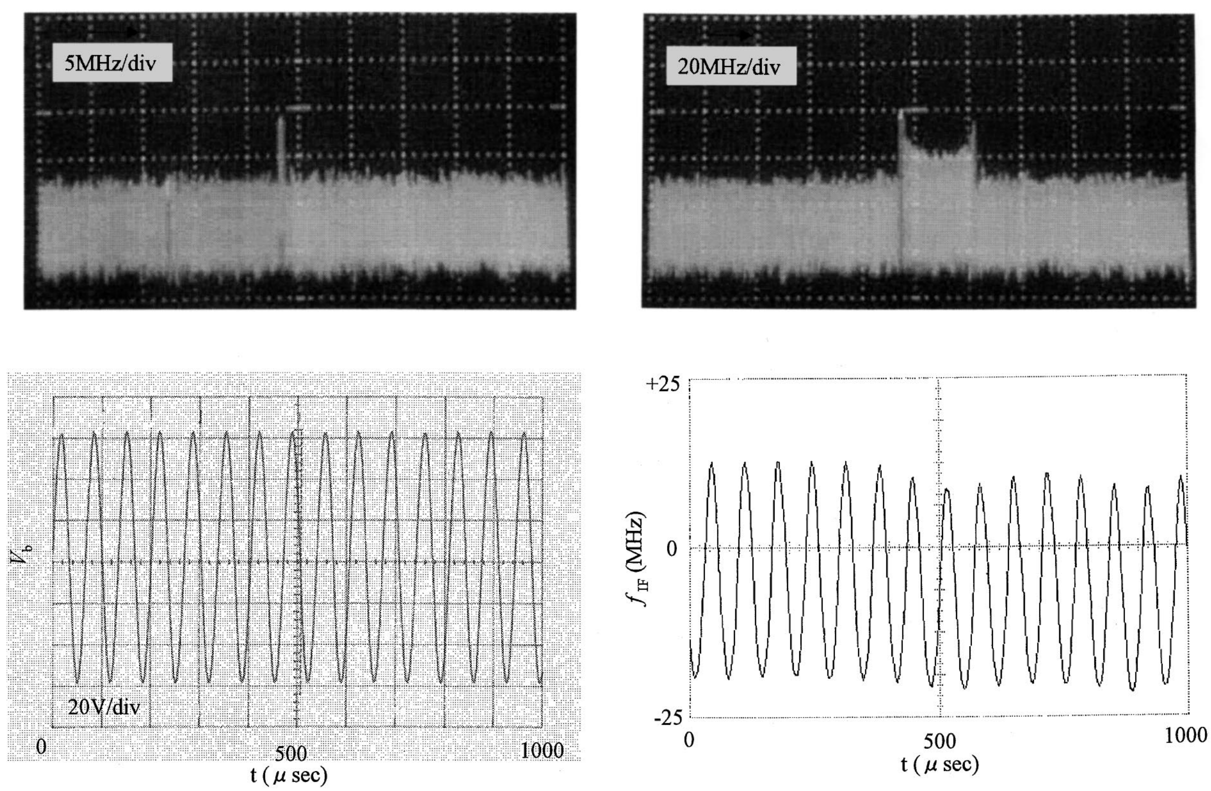

FIG. 4. Experimental results for frequency spectra without and with frequency modulation, for variation of body potential V_b, and for observed $f_{\rm IF}$; $f_m = 15$ kHz; $\Delta V_b = 120$ V; $\Delta f = 30$ MHz.

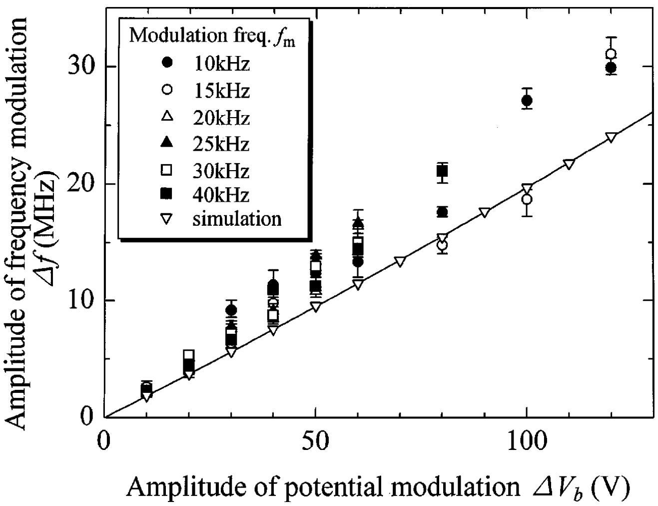

FIG. 5. Experimental and simulation results for frequency modulation amplitude Δf versus the amplitude of body potential modulation ΔV_b for $f_m = 10$, 15, 20, 25, 30, and 40 kHz; $\Delta f/\Delta V_b = 0.247 \pm 0.06$ MHz/V. Output power $P = 20$ W; other parameters the same as in Fig. 3.

distribution function for the interaction between an electron beam and a millimeter-wave field in the cavity [5,11,15–17,19–21]. A full scale simulation of that interaction would be required to determine $\varphi_{\rm eff}$, but it far exceeds the possibilities of our computers. An approximation modifying the methods [20] and [22] was adopted instead. The frequency modulation amplitude Δf from Eq. (3) was plotted for all φ values for both $\theta = 0$ and $\theta = \pi/2$. The intersection of such two plots gives us $\varphi_{\rm eff}$ and Δf. The simulation results presented in Fig. 5 by the solid line are in reasonable agreement with the experiment. We have also compared the experiment and the simulation for the output power variation presented by the lowest trace in Fig. 3. The average measured ratio of maximal to minimal power equals 1.6, whereas the simulation yields the ratio of the real parts of Eq. (1) for V_1 and V_2 with $\varphi = \varphi_{\rm eff}$ equal 1.56, so there is good agreement as well.

In summary, a frequency modulation amplitude up to several tens MHz have been achieved for a 300 GHz gyrotron output, whereas the modulation frequency applied to the accelerating voltage can be increased up to 40 kHz, and a linear dependence between the modulations of frequency and of accelerating voltage has been demonstrated.

The work was supported in part by a Grant-in-Aid from the Ministry of Education, Science, Sport and Culture of Japan. Thanks are due to Dr. G. F. Brand from School of Physics, University of Sydney, for invaluable discussions.

[1] T. Idehara, Y. Shimizu, K. Ichikawa, S. Makino, K. Shibutani, K. Kurahashi, I. Ogawa, Y. Okazaki, and T. Okamoto, Phys. Plasmas **2**, 3246 (1995).
[2] K. D. Hong, G. F. Brand, and T. Idehara, J. Appl. Phys. **74**, 5250 (1993).
[3] G. F. Brand, Int. J. Infrared Millim. Waves **16**, 879 (1995).
[4] O. Dumbrajs, J. A. Heikkinen, K. Sarparanta, S. K. Sipilä, K. Novik, and A. Piliya, Int. J. Infrared Millim. Waves **16**, 307 (1995).
[5] T. Idehara, Y. Shimizu, S. Makino, K. Ichikawa, T. Tatsukawa, I. Ogawa, and G. F. Brand, Phys. Plasmas **1**, 461 (1994); Int. J. Infrared Millim. Waves **18**, 391 (1997).
[6] G. Müller, V. Erckmann, M. Thumm, R. Wilhelm, D. Dorst, and W. Melkus, in *Proceedings of the 13th Symposium on Fusion Technology, Varese, 1984* (Pergamon, Oxford, 1984), pp. 811–816.
[7] E. Borie, G. Dammertz, O. Dumbrajs, G. Gantenbein, T. Geist, M. Kuntze, A. Möbius, H. U. Nickel, B. Piosczyk, and M. Thumm, in *Conference Digest of 16th International Conference on Infrared and Millimeter Waves, 1991, Lausanne, Switzerland* (The Society, Bellingham, WA, 1991), pp. 260–263.
[8] A. W. Fliflet, M. E. Read, K. R. Chu, and R. Seeley, Int. J. Electron. **53**, 505 (1982).
[9] T. Kariya, T. Saito, K. Kiwamoto, H. Gotoh, and S. Miyoshi, Jpn. J. Appl. Phys. **25**, 654 (1996).
[10] S. Alberti, M. Q. Tran, J. P. Hogge, T. M. Tran, A. Bondeson, P. Muggli, A. Perrenoud, B. Jödicke, and H. G. Mathews, Phys. Fluids B **2**, 1654 (1990).
[11] K. Hayashi and T. Sugawara, IEICE Trans. Electron. **E-75C**, 610 (1992).
[12] G. F. Brand, T. Idehara, T. Tatsukawa, and I. Ogawa, Int. J. Electron. **72**, 921 (1992).
[13] O. Dumbrajs and G. Nusinovich, IEEE Trans. Plasma Sci. **20**, 452 (1992).
[14] O. Dumbrajs and J. Heikkinen, Fusion Technol. **26**, 561 (1994).
[15] K. E. Kreischer, B. G. Danly, P. Woskoboinikow, W. J. Mulligan, and R. J. Temkin, Int. J. Electron. **57**, 851 (1984).
[16] R. M. Jones and M. W. Alcock, Int. J. Electron. **57**, 901 (1984).
[17] R. M. Jones and P. A. Lindsay, Int. J. Electron. **61**, 937 (1986).
[18] E. V. Zasypkin, Radiotekh. Elektron. **32**, 2599–2605 (1987).
[19] I. I. Antakov, E. V. Zasypkin, and E. V. Sokolov, Int. J. Infrared Millim. Waves **14**, 1001 (1993).
[20] G. F. Brand, in *Infrared and Millimeter Waves* (Academic Press, New York, 1985), Vol. 14, Chap. 6, pp. 371–408.
[21] G. S. Park, J. L. Hirshfield, and C. M. Armstrong, Int. J. Electron. **72**, 921 (1992).
[22] G. F. Brand, Int. J. Infrared Millim. Waves **4**, 919 (1983).